Microphase Separation Behavior on the Surfaces of Poly(dimethylsiloxane)-*block*-poly(2,2,3,3,4,4,4-heptafluorobutyl methacrylate) Diblock Copolymer Coatings

Zheng-Hong Luo, Hai-Jiang Yu, Wei Zhang

Department of Chemical and Biochemical Engineering, College of Chemistry and Chemical Engineering, Xiamen University, Xiamen 361005, People's Republic of China

Received 1 December 2008; accepted 22 March 2009
DOI 10.1002/app.30486
Published online 27 May 2009 in Wiley InterScience (www.interscience.wiley.com).

ABSTRACT: Microphase separation behavior on the surfaces of poly(dimethylsiloxane)-*block*-poly(2,2,3,3,4,4,4-heptafluorobutyl methacrylate) (PDMS-*b*-PHFBMA) diblock copolymer coatings was investigated. The PDMS-*b*-PHFBMA diblock copolymers were successfully synthesized via atom transfer radical polymerization (ATRP). The chemical structure of the copolymers was characterized by nuclear magnetic resonance and Fourier transform infrared spectroscopy. Surface composition was studied by X-ray photoelectron spectroscopy. Copolymer microstructure was investigated by atomic force microscopy. The microstructure observations show that well-organized phase-separated surfaces consist of hydrophobic domain from PDMS segments and more hydrophobic domain from PHFBMA segments in the copolymers. The increase in the PHFBMA content can strengthen the microphase separation behavior in the PDMS-*b*-PHFBMA diblock copolymers. And the increase in the annealing temperature can also strengthen the microphase separation behavior in the PDMS-*b*-PHFBMA diblock copolymers. Moreover, Flory-Huggins thermodynamic theory was preliminarily used to explain the microphase separation behavior in the PDMS-*b*-PHFBMA diblock copolymers. J Appl Polym Sci 113: 4032–4041, 2009

Key words: microphase separation behavior; PDMS-*b*-PHFBMA; AFM; Flory-Huggins thermodynamic theory

INTRODUCTION

The surfaces of polymers have strong influences on their performances such as anti-biofouling, biocompatibility, and antithrombogeneity.[1,2] The microphase separation behavior generally occurs on the surfaces of the block polymers and affects their performances.[2,3] In addition, surface energy is one of the most important properties of polymers. Function of polymers can be greatly affected by surface energy due to its special properties.[2–4] Siloxane polymers and fluorinated polymers are two families of low surface energy materials. There were lots of investigations focusing on modifying the surfaces of the polymers using siloxane polymers that have low surface energy or/and fluorinated polymers to obtain the surface microphase separation structures.[2–12]

Recently, Ku et al.[5] synthesized amorphous poly (imide siloxane)-*b*-polydimethylsiloxane (PIS-*b*-PDMS) dibolck copolymers by condensation polymerization and studied their microphase separation behavior on the surfaces. The results showed that the surface morphology and microphase separation of the diblock copolymers could be affected by the segmental length of PDMS. The surface morphology tended toward bicontinuous as the segmental length of PDMS increased, and the microphase separation of PIS-*b*-PDMS copolymer coating was driven and dominated by the PDMS segments.[5] Fang et al.[2] synthesized the block polymers containing PDMS segments by step condensation polymerization, namely, poly(ethylene glycol)-4,4′-diphenylmethanediisocyanate-polydimethylsiloxane(PEG-*b*-MDI-*b*-PDMS) triblock copolymers. The microphase separation on the surfaces of the triblock copolymers was observed. Fang et al.[2] disclosed that annealing of the copolymer films would strengthen the microphase separation. Furthermore, the surface morphology of the copolymer films could be controlled by the variations of the PDMS content and the chain length of PEG.[2] For fluorinated polymers, Saïdi et al.[6] prepared copolymers of styrene and fluorinated acrylate with F-octylalkyl,

Correspondence to: Z.-H. Luo (luozh@xmu.edu.cn).
Contract grant sponsor: National Natural Science Foundation of China; contract grant number: 20406016.
Contract grant sponsor: Nation Defense Key Laboratory of Ocean Corrosion and Anti-corrosion of China; contract grant number: 51449020205QT8703.
Contract grant sponsor: Fujian Province Science and Technology Office of China; contract grant number: 2005H040.

$F(CF_2)_8(CH_2)_n$ side groups by free-radical polymerization. Contact angle measurements revealed that the incorporation of a long perfluorocarbon side chain was an essential element of the molecular design for low surface energy materials.

Based on the above discussion, it is clear that past studies in this field are still limited to fluorinated polymers or polymers with PDMS segments. There are few reports on the studies of the block copolymers containing siloxane polymers and fluorinated polymers. We have synthesized a series of PDMS-*b*-PHFBMA diblock copolymers using commercially available materials by atom transfer radical polymerization (ATRP).[13] In addition, the PDMS-*b*-PHFBMA copolymers consist of two hydrophobic segments, namely, PDMS segment and PHFBMA segment. PDMS is hydrophobic and PHFBMA is even more hydrophobic than PDMS. However, past studies on the surface morphology of similar copolymers including two hydrophobic segments were absent. In this study, the microphase separation behavior on the surfaces of the PDMS-*b*-PHFBMA diblock copolymer was investigated. Moreover, Flory-Huggins thermodynamic theory was preliminarily used to explain the microphase separation behavior in the PDMS-*b*-PHFBMA diblock copolymers.

EXPERIMENTAL

Materials

Monocarbinol-terminated polydimethylsiloxane (PDMS-OH) and 2-bromo-2-methyl-propionylbromide (98%) were obtained from A Better Choice for Research Chemicals GmbH & Co. KG (ABCR), with the former having an average molecular weight of 5000 g/mol determined by gel permeation chromatograph (GPC), which was performed using THF as the eluent at a flow rate of 1 mL/min with a polystyrene standard as the reference. Triethylamine was supplied by Sinopharm Chemical Reagent Co, Ltd. (SCRC, 99%) and stored over 4-A° molecular sieves. *N*-Propylamine (98%) and pyridine-2-carboxaldehyde (99%) were obtained from ABCR GmbH & Co. KG. 2,2,3,3,4,4,4-Heptafluorobutyl methacrylate (HFBMA, 98%) purchased from Lancaster was washed with 5% aqueous NaOH solution to remove the inhibitor. Copper (I) bromide (98%) obtained from Aldrich was purified according to the method of Keller and Wycoff.[14] All other reagents and solvents were obtained from SCRC and used without further purification.

Synthesis of PDMS-*b*-PHFBMA diblock copolymers

The PDMS-*b*-PHFBMA diblock copolymers were synthesized based on our previous work.[13] The detailed procedures for the copolymerizations and analysis were described previously.[13] Here, we only describe the procedures briefly. First, bromine end-capped polydimethylsiloxane macroinitiator was synthesized as a macroinitiator of ATRP. *N*-(*n*-Propyl)-2-pyridinylmethanimine was prepared as the ligand for the CuBr catalyst. Then, the polymerization of HFBMA was conducted in a dry flask under an inert atmosphere of nitrogen. The typical HFBMA(M) polymerization proceeded with the molar ratio of each component of [M]/[I]/[CuBr]/[ligand] = 60 : 1 : 1 : 2. The deoxygenated PDMS-Br initiator, toluene, and HFBMA were added to the flask using degassed syringes. The solution was heated after three freeze-pump-thaw cycles, and then the *N*-(*n*-propyl)-2-pyridinalmethanimine ligand was added to the solution, stirred, and heated to 94°C by an oil bath. The synthetic scheme was shown in Scheme 1. The reaction was stopped after several hours by cooling the solution in ice bath. The final polymer was purified by passing the solution through a basic alumina column and by precipitating into methanol several times.

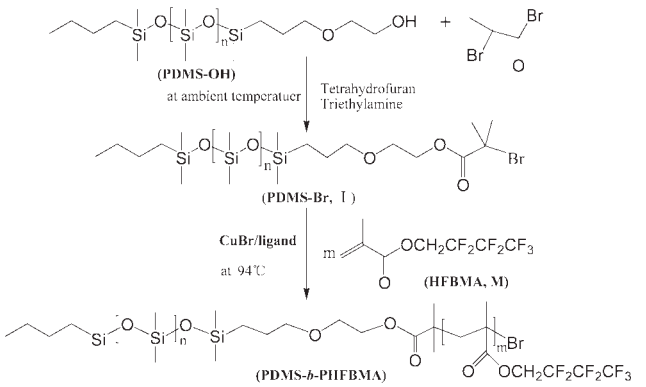

Scheme 1 Synthetic scheme for the preparation of PDMS-*b*-PHFBMA diblock copolymers.

Fourier transform infrared analysis

Fourier transform infrared (FTIR) analysis was performed on an Avatar 360 FTIR spectrometer (Nicolet Instruments, Madison, WI). The spectrum was recorded before 32 times scanning at a resolution of 4 cm^{-1}.

^1H nuclear magnetic resonance analysis

The samples were dissolved in deuterated chloroform (free of TMS), and the NMR spectra were measured on a Bruker AV400 NMR spectrometer.

Atomic force microscopy observation

Atomic force microscopy (AFM) observation was made on NanoScope SPM IIIa (Veeco, US) in ultra-light-tapping mode under ambient conditions (25°C, 40% RH), using the microfabrication cantilevers with a spring constant of approximately 20 Nm^{-1}. All AFM data including the topographical and the three-dimensional (3D) image as well were recorded simultaneously. The films for the AFM measurements were prepared with a single drop of copolymer solution in THF on freshly cleaned Si wafer. Thickness of the films is about 20–50 μm. The samples for AFM measurements were dried in vacuum at room temperature.

X-ray photoelectron spectroscopy

X-ray photoelectron spectroscopy (XPS) measurements were recorded with a PHI quantum 2000 scanning ESCA microprobe (physical electronic, US), equipped with an Al $K\alpha_{1,2}$ monochromatic source of 1486.60 eV. The beam was 200 μm in diameter and the analysis area was 1.5 mm × 0.2 mm. The measurements were typically operated at 35 W. A typical mutilplex pass energy was 29.35 eV, and a typical survey pass energy was 187.85 eV. The take-off angle was 45°. Narrow scan spectrometer of C 1s, O 1s, N s, and Si 2p were collected and peak analysis was carried out using software. The basic vacuum was 5×10^{-8} Pa, while XPS spectra were taken up at 5×10^{-7} Pa. XPS samples were prepared using the following methods. The block copolymers were dissolved in THF, then were casted onto freshly cleaned aluminum foil and dried in a vacuum at room temperature.

Contact angle and surface energy measurements

The contact angle and surface energy were obtained by SL-200B measurement (Suolun, China) since reported contact angle was an average of five individual measurements on different regions of the same sample. The films for contact angle and surface free energy measurements were prepared by casting the copolymer solution onto clean glass slides. All samples were dried in vacuum at room temperature for 24 h. The surface energy of the films was calculated by Owens–Wendt–Kaelble method. The equilibrium contact angle is well defined by Young's equation[2,15]:

$$\sigma_s = \sigma_{sl} + \sigma_l \cos\theta \quad (1)$$

where σ_s, σ_l, and σ_{sl} are the interfacial free energies at solid-vapor, liquid-vapor, and solid-liquid interfaces, respectively. θ is the contact angle of liquid on a solid surface. According to Refs. 2, 15, and 16, σ_s and σ_l can be expressed as follows:

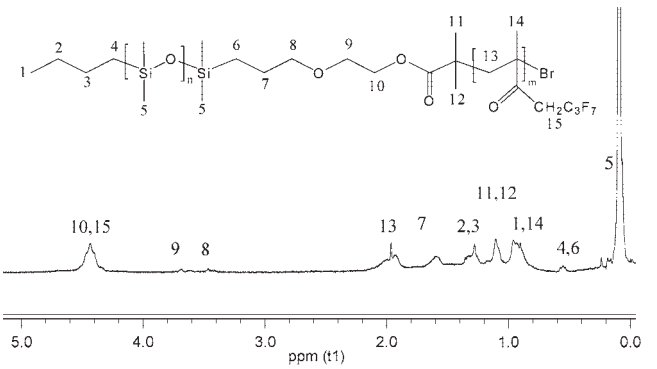

Figure 1 H NMR spectrum of PDMS-*b*-PHFBMA diblock copolymers (sample: No. 3 $DMS_{65}HFBMA_{9.7}$).

$$\sigma_s = \sigma_s^d + \sigma_s^p \quad (2)$$

$$\sigma_l = \sigma_l^d + \sigma_l^p \quad (3)$$

where σ_s^d and σ_s^p are the dispersive and polar contribution to the surface energy for the solid, σ_l^d and σ_l^p for the liquid, respectively. Accordingly, σ_{sl} can be calculated according to eq. (4). In this study, deionized water and ethylene glycol were selected as the probe liquid to determine the surface free energies of copolymer films.

$$\sigma_{sl} = \sigma_s + \sigma_l - 2\left(\sqrt{\sigma_s^d \sigma_l^d} + \sqrt{\sigma_s^p \sigma_l^p}\right) \quad (4)$$

RESULTS AND DISCUSSION

Synthesis of PDMS-*b*-PHFBMA diblock copolymers

A series of PDMS-*b*-PHFBMA diblock copolymers were first synthesized by ATRP to observe the surface properties of the PDMS-*b*-PHFBMA diblock copolymers, especially their microphase separation behavior. Concerning the synthesis and structure characterization of PDMS-*b*-PHFBMA diblock copolymers, readers are encouraged to refer to our past work.[13] Here, we only provide two typical results of the structural measurement including ^1H NMR and FTIR spectrum to keep this work integrate.

Typical ^1H NMR and FTIR spectra obtained in our group were shown in Figures 1–2, respectively. In Figure 1, there are two distinct peaks: one at 4.43 ppm, corresponding to hydrogen in the $-OCH_2(CF_2)_2CF_3$ group affected by both the ester group and the $-CF_2$ group, and the other at 0.05 ppm corresponding to hydrogen on dimethylsiloxane repeat units. In addition, Figure 1 shows that

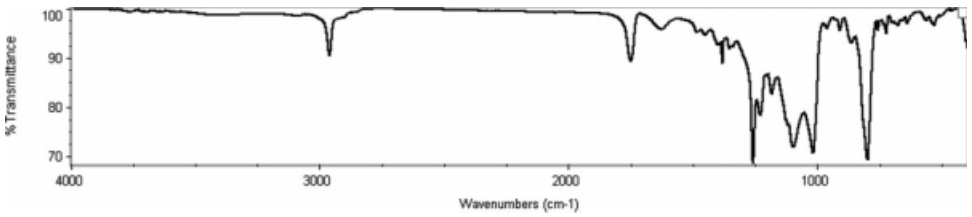

Figure 2 FTIR spectra of PDMS-*b*-PHFBMA diblock copolymers (sample: No. 3 $DMS_{65}HFBMA_{9.7}$).

the PDMS polymers have distinctive peaks, centered at 0.05 ppm in the ^1H NMR spectrum, corresponding to the dimethylsiloxane repeat units. Integral ratios of the two regions can be used to calculate the absolute number-average molecular weight (M_n) values for the diblock copolymers. From the FTIR spectroscopy at 1743 cm^{-1} corresponding to the ester group shown in Figure 2, we can also ascertain that the copolymer PDMS-*b*-PHFBMA has been successfully synthesized. Two peaks, centered at 1228 and 1182 cm^{-1}, correspond to the symmetric and antisymmetric stretching vibrations of the $-CF_2$ group, respectively.[17] There are two medium bands at 563 and 726 cm^{-1}, corresponding to a combination of the cocking and wagging vibrations of the $-CF_3$ group.[18] The characteristic peaks of the PDMS block appear between 1022 and 1112 cm^{-1}.[13] Consequently, the measuring results prove that the PDMS-*b*-PHFBMA diblock copolymers were successfully synthesized.

Microphase separation behavior

Figure 3 illustrates the typical AFM images of the diblock copolymer $DMS_{65}HFBMA_{13.65}$ films. The rough topography and three-dimensional (3D) image exhibited across surface are believed to be the result of the phase separation. It is well known that PDMS is hydrophobic and fluorine-containing polymer is even more hydrophobic than PDMS. In the case of ultra-light-tapping mode, the interaction largely depends on a meniscus force on the polymer surface, i.e., hydrophilicity (hydrophobicity) and wettability. Because the hydrophobic patches appear as low spots and the less hydrophobic areas as high spots,[2,15,19] the phase data for the hydrophobic patches are bright and the less hydrophobic areas are dark in the AFM topographical data obtained under ultra-light-tapping mode,[20,21] the topography image in Figure 3 displays a high-resolved phase interface where dark patches were the hydrophobic PDMS domains, and bright phase were the more hydrophobic PHFBMA domains. In addition, we can also obtain the following data via using the software along with NanoScope SPM IIIa: the average height of the protuberant area in Figure 3(B) is 10 nm, the size of the distribution phase area is about 30 to 50 nm, and root mean square roughness in an area of 1000×1000 nm^2 of this sample is 3.633 nm.

Effects of PHFBMA content

Figures 3, 4 and 5 describe the AFM phase images of the diblock copolymer films with different compositions. With the increase in the PHFBMA content, the surface pattern changes from a structure of the

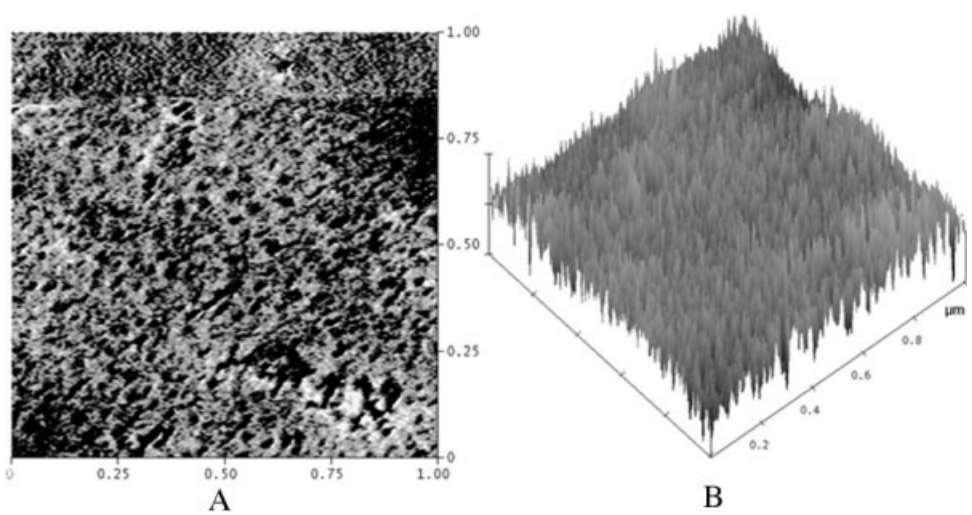

Figure 3 The AFM phase image and 3D image of $DMS_{65}HFBMA_{13.65}$ copolymer films (No. 1 $DMS_{65}HFBMA_{13.7}$) (A, AFM phase image; B, 3D image).

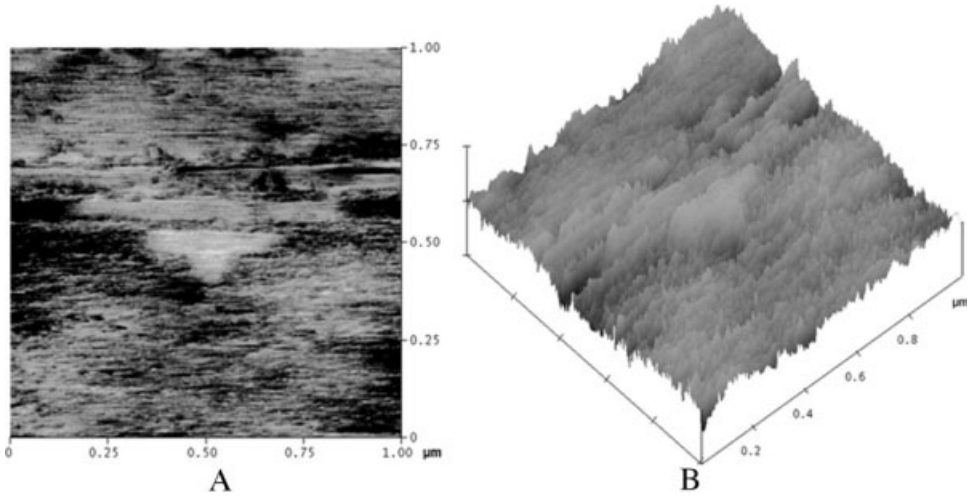

Figure 4 The AFM phase image and 3D image of $DMS_{65}HFBMA_{11.70}$ copolymer films (No. 2 $DMS_{65}HFBMA_{11.7}$) (A, AFM phase image; B, 3D image).

hydrophobic PDMS-rich domain surrounded by the more hydrophobic PHFBMA (Fig. 5), to inter-penetration network pattern (Fig. 3). Simultaneously, the roughness data computed by software along with NanoScope SPM IIIa (Table I) show that the roughness of the sample increases with the increase in the PHFBMA content.

The evolution of the surface morphology with the increase in the polymerization degree of PHFBMA can be caused by the enrichment of PHFBMA segments at the copolymer–air interface and the reorganization of PDMS phase, which can also be further confirmed by XPS detection. The XPS images of the three samples listed in Table I are obtained. All XPS images are very alike with each other and represent different surface atomic ratios of Si/F computed by software. Accordingly, here we only supply the typical XPS images of Sample 1. The XPS images and detailed discussion regarding the surface compositions of the PDMS-*b*-PHFBMA diblock copolymer samples are shown in Figure 6. Figure 6(A) is a broad scan of the binding energy (BE) spectrum from 0 to 960 eV for $DMS_{65}HFBMA_{13.65}$ diblock copolymer film (Sample 1 in Table I). It comprises four strong peaks and three weak peaks at approximately 835, 687, 532, 285, 152, 102, and 32 eV that result from direct photoionization from F KLL, F 1s, O 1s, C 1s, Si 2s, Si 2p, and F 2s core levels, respectively. The high-resolution C 1s spectrum [Fig. 6(B)] of $DMS_{65}HFBMA_{13.65}$ diblock copolymer film exhibits five peaks. The component with BE at 284.7 eV is attributed to the —C—H species. Two peaks at 288.4 and 290.0 eV are assigned to the —C—O— species and —O—C=O— species of $DMS_{65}HFBMA_{13.65}$ diblock copolymers, respectively. The component with BE at 292.1 eV is ascribed to $—CF_2$ group, and

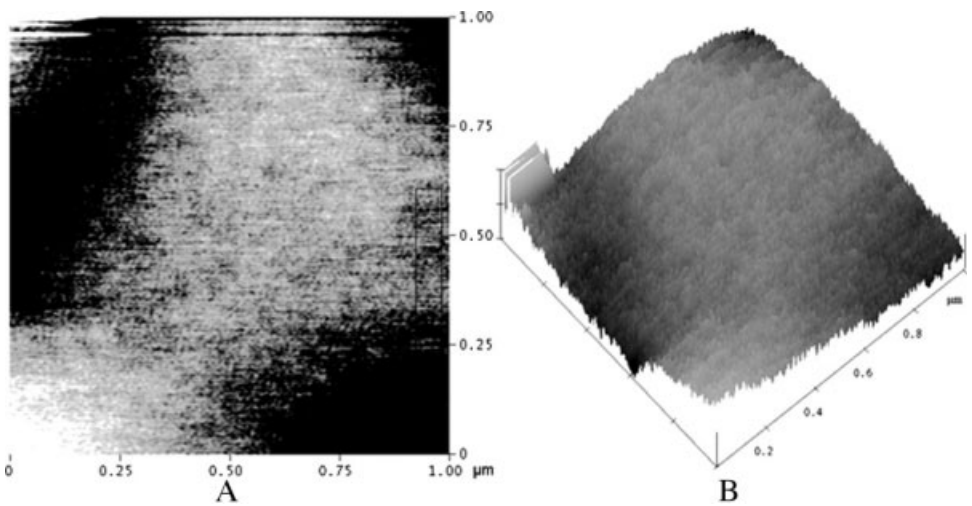

Figure 5 The AFM phase image and 3D image of $DMS_{65}HFBMA_{9.7}$ copolymer films (No. 3 $DMS_{65}HFBMA_{9.7}$) (A, AFM phase image; B, 3D image).

TABLE I
The Surface Compositions and Roughness of PDMS-*b*-PHFBMA Diblock Copolymers Dependent on the PHFBMA Content[9]

Samples no.	DMS_xHFBMA_y	W_{PHFBMA}[a] (%)	$M_{n,theo}$[b] (g/mol)	$M_{n,NMR}$[c] (g/mol)	$M_{n,GPC}$[d] (g/mol)	PDI[e]	Si/F[f]	Roughness[g] (nm)
1	$DMS_{65}HFBMA_{13.7}$	43.3	7500	7300	7412	1.23	3.06	3.633
2	$DMS_{65}HFBMA_{11.7}$	39.5	7200	6950	7107	1.20	3.36	2.247
3	$DMS_{65}HFBMA_{9.7}$	35.1	6900	6800	6891	1.13	4.42	1.279

[a] W_{PHFBMA} represents the weight percent of the PHFBMA block calculated by the equation: PHFBMA % = (287 × DP_n)/(5150 + 287 × DP_n), 287 is the molecular weight of HFBMA, DP_n is the degree of polymerization of the PHFBMA segment, 5150 is the molecular weight of PDMS-Br macroinitiators measured by GPC, which was performed using THF as the eluent at a flow rate of 1 mL/min with a polystyrene standard as the reference.
[b] $M_{n,theo}$ represents the theoretical molecular weight.
[c] The molecular weight was measured by ^1H NMR (two distinctive peaks in the ^1H NMR spectrum (Fig. 1) can be assigned to hydrogen of the $-OCH_2-$ group at 4.43 ppm affected by the ester group and the dimethylsiloxane repeat units at 0.0–0.2 ppm. Integral ratio of the two regions can be used to calculate number-average molecular weight (M_n) values: $M_n = 5150 + 287 \times DP_n$).
[d] $M_{n,GPC}$ represents the molecular weight measured by GPC.
[e] The polydispersity of the copolymer was measured by GPC which was performed using THF as the eluent at a flow rate of 1 mL/min with a polystyrene standard as the reference.
[f] The surface atomic ratio of Si/F of the copolymer films was determined by XPS.
[g] The roughness of the copolymer films was obtained via the AFM software.

the peak at 294.5 eV results from $-CF_3$ species. The atom contents of C 1s, O 1s, Si 2p, and F 1s can be computed by the software along with the XPS apparatus. Furthermore, Table I lists the surface atomic ratio of Si/F of the copolymer films determined by XPS. The data show that the surface atomic ratio of Si/F decreases with the increase in the polymerization degree of PHFBMA, which indicates the enrichment of PHFBMA segments since F is only in the PHFBMA segments and Si only in the PDMS segments.

Effect of annealing treatment

Here, we should point out that there is no change in the structure of the sample before and after the annealing treatment. It can be proved by the FTIR and XPS characterizations. The FTIR spectra of the PDMS-*b*-PHFBMA diblock copolymer samples in this study were shown in Figure 7. It was proved in Figure 7 that the annealing treatment could not alter the structures of the samples. In fact, all peak positions of curves a–d in Figure 7 are the same as the peak positions of the curve in Figure 2. There are only differences in the peak intensity. However, the annealing treatment can affect the surface compositions of the copolymer films.

Figures 8–10 display the surface morphology of the same sample as in Figure 5 dependent on annealing under vacuum at 60, 90, and 120°C for 2 h, respectively. From Figures 8–10, we can see that more hydrophobic segments seem to immigrate to the surface to form layer-like structure. Accordingly, more distinct phase interfaces are observed with the

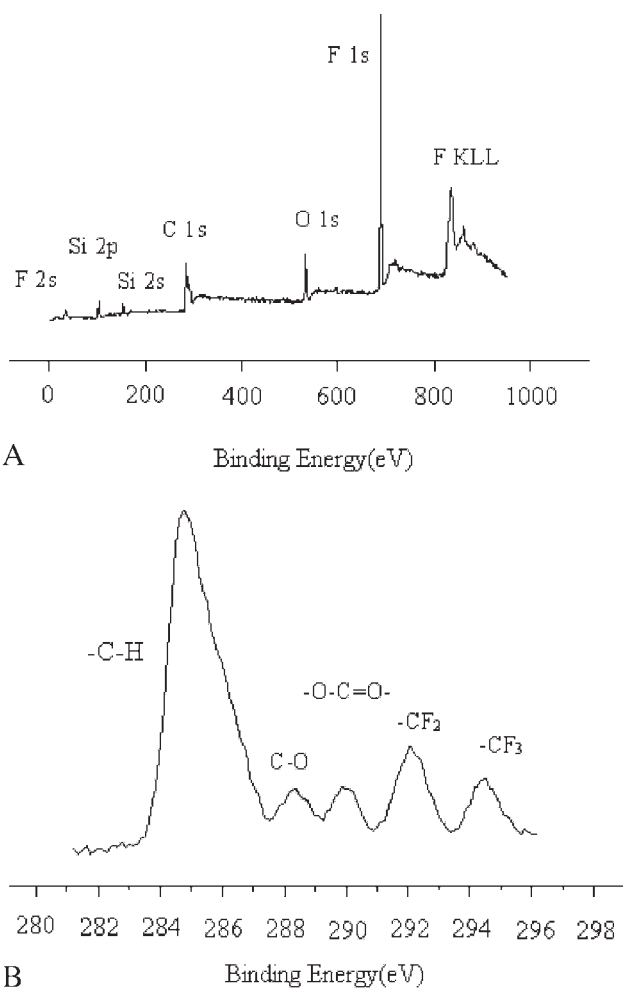

Figure 6 XPS of $DMS_{65}HFBMA_{13.65}$ copolymer films (No. 1 $DMS_{65}HFBMA_{13.7}$) (A, broad scan of the BE spectrum; B, high-resolution C 1s spectrum).

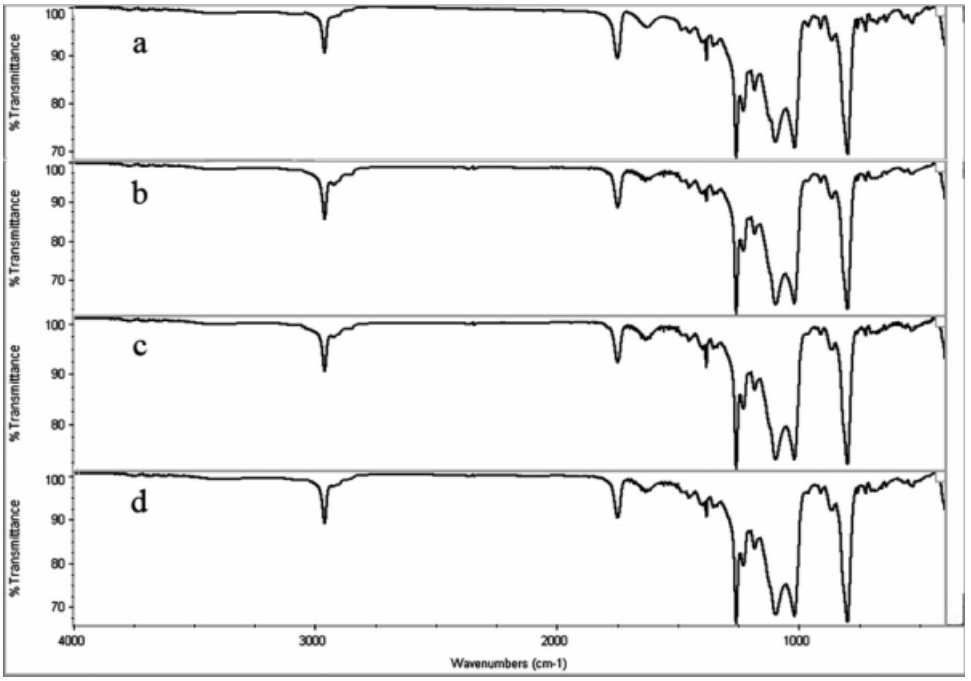

Figure 7 FTIR spectra of PDMS-*b*-PHFBMA diblock copolymers dependent on the annealing treatment (a, No. 3 $DMS_{65}HFBMA_{9.7}$, unannealed; b, No. 4 $DMS_{65}HFBMA_{9.7}$, annealed at 60°C; c, No. 5 $DMS_{65}HFBMA_{9.7}$, annealed at 90°C; d, No. 6 $DMS_{65}HFBMA_{9.7}$, annealed at 120°C).

increase in annealing temperature according to Figures 8–10, which suggests that further segment segregation happens during annealing. Simultaneously, the computed roughness data (Table II) show that the roughness of the sample increases with the increase in the annealing temperature.

The evolution of the surface morphology dependent on annealing may be caused by the enrichment of PHFBMA segments at the copolymer–air interface and the reorganization of hydrophilic phase, which is further confirmed by XPS detection. The XPS images of the three samples shown in Table II are also obtained. Because the XPS images of Samples 2 and 3 are very alike to the images of Sample 1 they are not supplied in this study. However, we compute the surface atomic ratio of Si/F of the copolymer films before and after annealing determined by XPS. Table II shows that the atomic ratio of Si/F of the copolymers decreases after annealing, indicating the enrichment of PHFBMA segments at

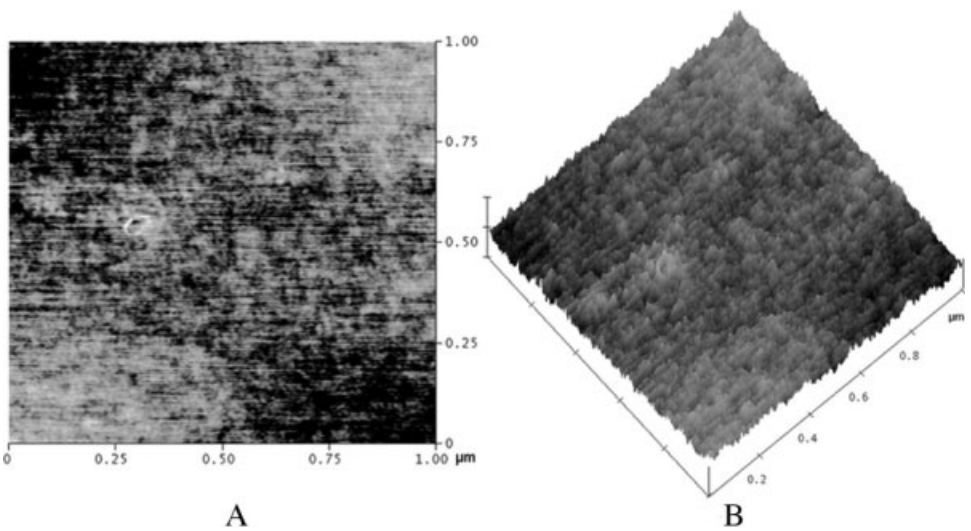

Figure 8 The AFM phase image and 3D image of $DMS_{65}HFBMA_{9.7}$ copolymer films annealed under vacuum at 60°C for 2 h (No. 4 $DMS_{65}HFBMA_{9.7}$, annealed at 60°C) (A, AFM phase image; B, 3D image).

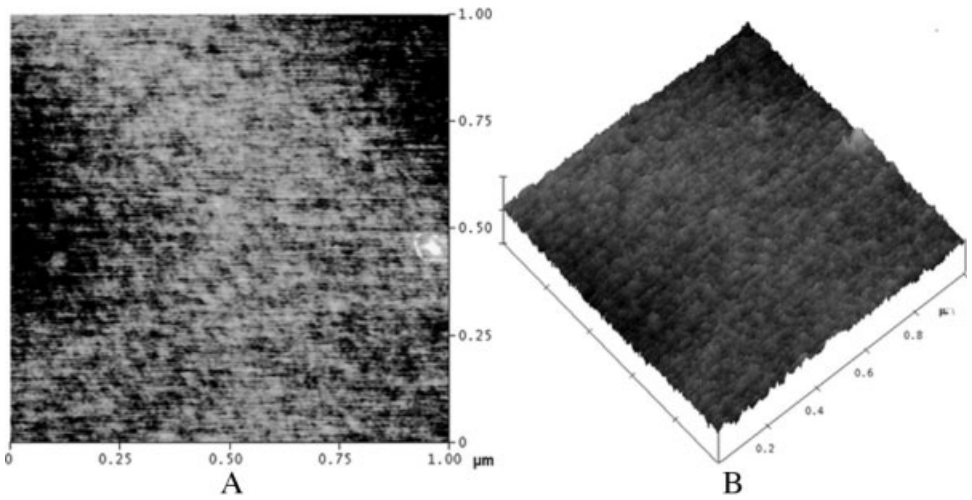

Figure 9 The AFM phase image and 3D image of $DMS_{65}HFBMA_{9.7}$ copolymer films annealed under vacuum at 90°C for 2 h (No. 5 $DMS_{65}HFBMA_{9.7}$, annealed at 90°C) (A, AFM phase image; B, 3D image).

high temperature. This is because PHFBMA has a lower surface tension and migrates to the surface. However, PHFBMA segments cannot cover the whole surface because the immigration of PHFBMA segments is meanwhile restricted by the PDMS domain.

In addition, comparing Table II with Table I, we obtain that the roughness of the samples is not proportional to the atomic ratio of Si/F of the copolymers.

Surface energies of diblock copolymer films

The total surface energies (σ_s) along with the polar and dispersive contributions to the surface energy of the diblock copolymers with different polymerization degrees and annealing temperatures are determined and summarized in Table III. Compared with the surface energies of the block copolymer films, it is obvious that all the diblock copolymer films provide a surface energy of as low as 19–25 mN/m. And the contact angle increases with the increase in polymerization degree of PHFBMA and annealing temperature.

Obviously, such low surface energy can be related to the surface microphase separation of the diblock copolymers. In our opinion, microphase separation makes the low surface energy parts in the bulk tend to segregate to the surface, results in more fluorine enrichment and gives stronger hydrophobicity. In practice, one knows that the block copolymer exhibits the microphase-separated structure with a nanometer size because two different block sequences are chemically connected to each other, resulting in that each component cannot form large domains. Thus, the size of microphase-separated structure is

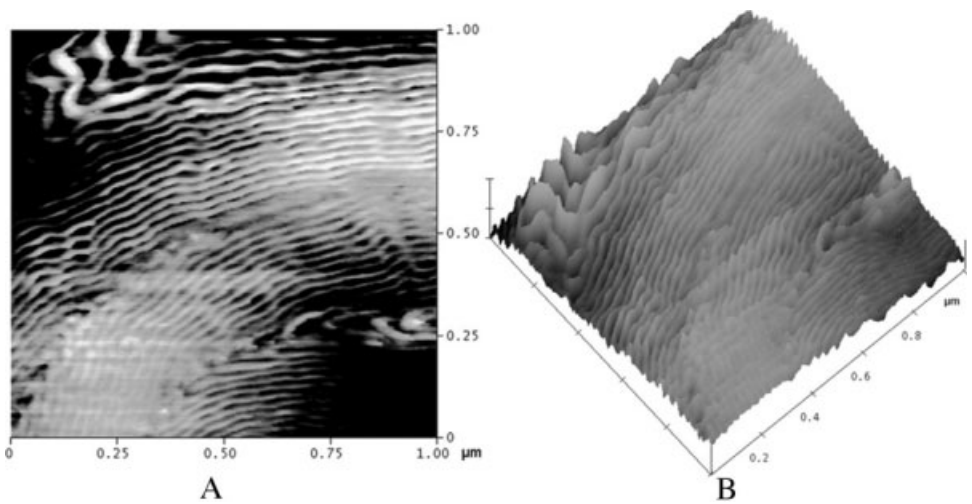

Figure 10 The AFM phase image and 3D image of $DMS_{65}HFBMA_{9.7}$ copolymer films annealed under vacuum at 120°C for 2 h (No. 6 $DMS_{65}HFBMA_{9.7}$, annealed at 120°C) (A, AFM phase image; B, 3D image).

TABLE II
The Surface Compositions and Roughness of PDMS-*b*-PHFBMA Diblock Copolymers Dependent on the Annealing Temperature

Samples no.	DMS_xHFBMA_y	Annealing temperature (°C)	Si/F[a]	Roughness[b] (nm)
3	$DMS_{65}HFBMA_{9.7}$	Unannealed	4.42	1.279
4	$DMS_{65}HFBMA_{9.7}$	60	4.20	1.356
5	$DMS_{65}HFBMA_{9.7}$	90	4.16	1.974
6	$DMS_{65}HFBMA_{9.7}$	120	4.00	2.970

[a] The surface atomic ratio of Si/F of the copolymer films was determined by XPS.
[b] The roughness of the copolymer films was obtained via the AFM software.

controllable by change in the segmental length of each block. The structure itself as well as the size of microphase-separated domains can also be controlled by the ratio of two block sequences, and annealing temperature.[3,22] Accordingly, it is the reason why surface energy of the PDMS-*b*-PHFBMA diblock copolymers is as low as 19–25 mN/m.

Thermodynamic analysis of microphase separation

In the present work, the surface measurements of all the above samples including the AFM observation are done at room temperature (298 K), although the annealing temperatures differ from 298 K. In practice, the annealing temperature only affects the surface compositions of the copolymer films. Therefore, we here discuss the microphase separation behavior preliminarily in the PDMS-*b*-PHFBMA diblock copolymers at room temperature according to Flory-Huggins thermodynamic theory.

The miscibility of hard and soft segments can be estimated by Flory-Huggins interaction parameter[23,24]:

$$\chi_{h,s} = \chi_{\Lambda s} + V_r(A_h - A_s)^2/(RT) \quad (5)$$

where $\chi_{h,s}$ is the miscibility of hard and soft segments in block copolymer, V_r is the reference volume, A_h and A_s are the solubility parameters of hard and soft segments, respectively, R is the gas constant, T is absolute temperature, $\chi_{\Lambda s}$ is the entropy term and can be neglected for polymer blends. Thus, we can obtain eq. (6)[23,24]:

$$\chi_{h,s} = (A_h - A_s)^2/6 \quad (6)$$

for $T = 298$ K, with RT in calories, and the V_r taken as 100 cm^3/mol.[23,24] As for eqs. (5) and (6), readers are encouraged to refer to Refs. 23 and 24.

Although the quantitative use of $\chi_{h,s}$ may be questionable for block copolymers, it still allows us to analyze the phase separation behavior of diblock polymers. As to A_h and A_s, even though there is a well-know uncertainty in solubility parameters, relatively good estimates can be obtained from certain Refs. 3, 23, and 24. If $\chi_{h,s}$ is greater than 3, the block copolymer has microphase separation structure. Otherwise, the copolymer has no microphase separation structure.[3,23] According to past studies where the system is close to the PDMS-*b*-PHFBMA block copolymers examined in this study,[3,23,24] we can know that A_s of PDMS is about 7.46, and A_h of PHFBMA is nearly 13.2. The value of $\chi_{h,s}$ computed from eq. (6) is about 5.5, which is greater than 3 obviously. Therefore, the PDMS-*b*-PHFBMA block copolymers prepared in our group have a microphase separation structure. Further studies on incorporating surface energy considerations into Flory-Huggins thermodynamic theory to describe the microphase separation behavior on the surfaces of PDMS-*b*-PHFBMA diblock copolymers are in progress.

TABLE III
The Static Water Contact Angles of the PDMS-*b*-PHFBMA Diblock Copolymers Dependent on the PHFBMA Content and the Annealing Temperatures

Samples no.	DMS_xHFBMA_y	Annealing temperature (°C)	$\theta_{(H_2O)}$ (°)	σ_s[a] (mN/m)
1	$DMS_{65}HFBMA_{13.65}$	Unannealed	96.36	19.79
2	$DMS_{65}HFBMA_{11.70}$	Unannealed	92.66	22.06
3	$DMS_{65}HFBMA_{9.7}$	Unannealed	87.42	25.34
4	$DMS_{65}HFBMA_{9.7}$	60	91.04	23.06
5	$DMS_{65}HFBMA_{9.7}$	90	92.79	21.98
6	$DMS_{65}HFBMA_{9.7}$	120	93.57	20.78

[a] The values are obtained form a telescopic goniomete (SL-200B), and σ_s represents the surface energy of the PDMS-*b*-PHFBMA film.

CONCLUSIONS

Microphase separation behavior on the surfaces of PDMS-*b*-PHFBMA diblock copolymers was studied via AFM. The results prove that the diblock copolymers are well-defined polymers with microphase separation surfaces consisting of hydrophobic domain from PDMS segments and rather more hydrophobic domain from PHFBMA segments. In addition, the effects of the PHFBMA content and annealing temperature on the microphase separation behavior were investigated. The results show that the increases in the PHFBMA content and the annealing temperature can strengthen the microphase separation in PDMS-*b*-PHFBMA diblock copolymers. Furthermore, we preliminarily apply Flory-Huggins thermodynamic theory to explain the microphase separation behavior in PDMS-*b*-PHFBMA diblock copolymers. The microphase separation surface structures in the PDMS-*b*-PHFBMA diblock copolymers can also be proved according to Flory-Huggins thermodynamic theory.

References

1. Yebra, D. M.; Kill, S.; Johansen, K. D. Prog Org Coat 2004, 50, 75.
2. Fang, H. X.; Zhou, S. X.; Wu, L. M. Appl Surf Sci 2006, 253, 2978.
3. Olemskoi, A.; Savelyev, A. Phys Rep 2005, 419, 145.
4. Luo, Z. H.; Yu, H. J.; He, T. Y. J App Polym Sci 2008, 108, 1201.
5. Ku, C. K.; Lee, Y. D. Polymer 2007, 48, 3565.
6. Saïdi, S.; Guittard, F.; Guimon, C.; Géribaldi, S. Eur Polym J 2006, 42, 702.
7. Majumdar, P.; Webster, D. C. Macromolecules 2005, 38, 5857.
8. Gudipati, C. S.; Greenlief, C. M.; Johnson, J. A.; Prayongpan, P.; Wooley, K. L. J Polym Sci A Polym Chem 2004, 42, 6193.
9. Hosoya, A.; Kurakami, G.; Narita, T.; Hamana, H. React Func Polym 2007, 67, 1187.
10. Yang, C. P.; Su, Y. Y.; Chiang, H. C. React Func Polym 2006, 66, 689.
11. Li, H.; Zhang, Z. B.; Hu, C. P.; Ying, S. K.; Wu, S. S.; Xu, X. D. React Func Polym 2003, 56, 189.
12. Person, D. V.; Fitch, J. W.; Cassidy, P. E.; Kono, K.; Reddy, V. S. React Func Polym 1996, 30, 141.
13. Luo, Z. H.; He, T. Y. React Func Polym 2008, 68, 931.
14. Keller, R. N.; Wycoff, H. D. Inorg Synth 1947, 2, 1.
15. Owens, D. K.; Wendt, R. C. J Appl Polym Sci 1969, 13, 1741.
16. Kaelble, D. H. J Adhes 1970, 2, 66.
17. Brantley, E. L.; Jennings, G. K. Macromolecules 2004, 37, 1476.
18. Hozumi, A.; Kakinoki, N.; Asai, Y.; Takai, O. J Mater Sci Lett 1996, 15, 675.
19. Tan, H.; Guo, M.; Du, R. N.; Xie, X. Y.; Li, J. H.; Zhong, Y. P.; Fu, Q. Polymer 2004, 45, 1647.
20. Sauer, B. B.; Mclean, R. S.; Thomas, R. R. Langmuir 1998, 14, 3045.
21. Brandsch, R.; Bar, G.; Whangbo, M. H. Langmuir 1997, 13, 6349.
22. Kojio, K.; Uchiba, Y.; Mitsui, Y.; Furukawa, M.; Sasaki, S.; Matsunaga, H.; Okuda, H. Macromolecules 2007, 40, 2625.
23. Pascault, J. P.; Camberlin, Y. Polym Commun 1986, 27, 272.
24. Camberlin, Y.; Pascault, J. P. J Polym Sci Polym Phys Ed 1984, 22, 1835.